VISUALIZATION OF THE FLOW DISTRIBUTION INSIDE THE PISTON DISPLACEMENT OF A GAMMA-TYPE STIRLING ENGINE

J. Luis Luviano-Ortiz, C. Ulises Gonzalez-Valle, Guillermo Hernandez-Cruz,
Eduardo Ramos, Abel Hernandez-Guerrero, Sindy Tarazona-Cardenas*
Department of Mechanical Engineering,
University of Guanajuato,
Salamanca, Guanajuato,
Mexico
E-mail: abel@ugto.mx

ABSTRACT

The dynamics of the confined flow inside the piston displacement of a Gamma-type Stirling engine operating as a heat pump is experimentally analyzed. The diameter of the piston is 30 mm; 2 mm smaller than the internal diameter of the cold cylinder. As the piston performs its reciprocating motion, the gas leaks around the gap between the piston and the cylinder wall, generating a continuous pulsating motion. In the first part of the cycle air is introduced and compressed by the piston motion, and then the second part of the cycle starts by expanding the air and ejecting it from the assembly chamber. Experimental observations were carried out at frequencies in the range 100 to 300 rpm. The flow was visualized using a vertical laser beam plane oriented in the same axial direction of the piston's motion. The particles used as trackers are water drops condensed on carbon dioxide microcrystals. Images were taken with a high speed video camera with a frame rate of 1000 fps. PIV techniques were implemented to identify the flow main structures. For analysis purposes, fixed phase averages of the velocity fields are required, due to the turbulent regime observed in this phenomena and its oscillatory nature. Based on experimental measurements it can be demonstrated that the average flow involved is not axisymmetric, although very interestingly, specific inlet and exit regions of the piston-cylinder gap were identified.

INTRODUCTION

Stirling engines are thermal devices that are able to transform heat into mechanical work in a very efficient cycle. This can be achieved by forming a Stirling thermodynamic cycle between a heat source and a heat sink. As a thermal machine its efficiency is restricted by the Carnot efficiency, both are theoretically equal but in practice this efficiency value cannot be achieved.

The ideal Stirling cycle includes two isothermal processes and two constant volume processes. Theoretically the absorption and rejection of heat are carried out at constant temperature. Along the thermodynamic cycle the volume inside the chamber changes due the pistons motion and heat is transferred simultaneously. This kind of devices can be used as an engine or as a heat pump. For the heat pump operation an external driven force must be implemented. Several motion mechanisms can be used to drive this device. The motion mechanisms include rhombic drive, cam-drive, mass/spring thermal auto oscillations systems or swash plate drive [1]. A different dynamic behavior can be achieved by the implementation of each system.

There are several types of Stirling engines. The Gamma-type is one of the most common and widely studied Stirling engines. The Gamma-type configuration has two cylinders; displacer and power piston are used (similar to Beta-type engines). This configuration allows a complete separation between the displacer, where the heat exchange occurs, and the expansion chamber where the power piston is located [2]. The device analyzed in this study is a commercial Stirling Engine G U10050 manufactured by 3B SCIENTIFIC® PHYSICS [3,4].

NOMENCLATURE

X	[m]	Displacer displacement
R	[m]	Crank length
L	[m]	Rod length
U	[m s^{-1}]	Displacer linear velocity
A	[m s^{-2}]	Displacer acceleration
T	[s]	Time

Special characters

ω	[rad s^{-1}]	Angular velocity
θ	[rad]	Crank angle

A Particle Image Velocimetry (PIV) technique is implemented to visualize the fluid response inside the displacer. This type of procedure allows to determine important parameters and to picture some important phenomena effected inside the studied area. Several PIV techniques have been carried out throughout numerous experimental analyses. A PIV technique involves little particles that are tracked over time along the structure that needs to be analyzed, thus the local velocity of the fluid can be determined [5]. Quite a few particles can be used as trackers. Table 1 presents the main seeding materials implemented for liquid and gases. In this work a novel PIV technique is implemented; this PIV technique seeds dry ice particles as trackers. A few works implementing this technique are reported in the technical literature [6-8]. An important factor to take care of is the clarity of the obtained images; this technique allows very clear shoots. Regularly air PIV is done by seeding particles such glycerin due its refraction index [9]. The refraction index of this material is nearly equal to the glass, allowing the light to pass through the visualized area without suffering any diffraction. Although this effect the

glycerin is not the adequate tracker particle due the soiling caused inside the chamber of the pistons. So, due to its cleanliness the dry ice is selected as the tracker particle in this study.

Table 1. - Main seeding materials for liquid and gases visualization [5].

Seeding materials for liquid flows.		
Type	**Material**	**Mean diameter [µm]**
Solid	Polystyrene	10-100
	Aluminum flakes	2-7
	Hollow glass spheres	10-100
	Granules for synthetic coatings	10-500
Liquid	Different oils	50-500
Gaseous	Oxygen bubbles	50-1000
Seeding materials for gas flows.		
Type	**Material**	**Mean diameter [µm]**
Solid	Polystyrene	0.5-10
	Alumina Al_2O_3	0.2-5
	Titania TiO_2	0.1-5
	Glass micro-spheres	0.2-3
	Glass micro-balloons	30-100
	Granules for synthetic coatings	10-50
	Dioctylphathalate	1-10
	Smoke	<1
Liquid	Different oils	0.5-1.5
	Di-ethyl-hexyl-sebacate (DEHS)	0.5-1.5
	Helium-filled soap bubbles	1000-3000

In this work the complete instrumentation of a Gamma-type Stirling engine was carried out. Temperature, pressure and acceleration measurements were taken and reported. A simple kinetic analysis was developed and compared with the experimental data reported presenting a good accuracy with the experimental results. Flow visualization of the displacer is presented and discussed for several positions of the piston.

RESEARCH DESCRIPTION

The main purpose of this work lies in the instrumentation of a Gamma-type Stirling engine as well as the implementation of a Particle Image Velocimetry technique used when the device is operated as a heat pump. A commercial Stirling engine model U10050 [3] is used and shown in the Figure 1.

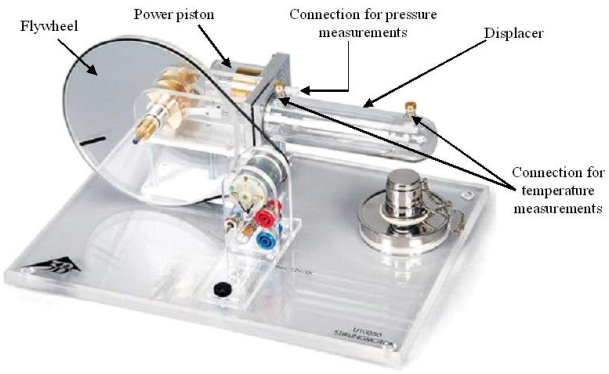

Figure 1 Stirling Engine U10050 [3].

This device has two connections mounted on the piston stroke for temperature measurements and a connection on the opposite side of the power piston in order to measure pressure inside the chamber. This set up is shown in Figure 1. The volume of the internal piston chamber is approximately 35 ml.

As mentioned before, the Stirling engine is operated as a heat pump by coupling the Stirling device to a DC motor. The DC motor velocity is controlled by an interface between the device, a power source (Agilent E3632A), and a CPU; in order to achieve the correct configuration it was necessary to build an encoder. The encoder allows the communication of the angular velocity value to the CPU through a data acquisition card NI USB-6008. While data was acquired through the DAQ, the CPU indicated the power source the adequate amount of voltage provided to the DC motor for maintaining a proper mean angular velocity (ω). These processes were taken through a LabView® interface.

The displacement of the MAIN piston was measured by an accelerometer (Arduino MPU6050) connected to a data acquisition card NI USB-8452. For the pressure variations measurements an Omega Engineering PX-105 transducer was used. For temperature measurements two type-T thermocouples were implemented. These three measuring devices were installed through a data acquisition card NI PCI-6040E connected to the CPU. The sensing interval used in the accelerometer, the pressure transducer, and the thermocouples is $\Delta t=0.001$ s, assuring enough experimental information since the mean angular velocity of the Stirling engine was 200 rpm.

Once the experimental data from the accelerometer was obtained, this data is integrated, once for velocity and twice for displacement of the power piston. Following the gamma configuration of the Stirling engine it is well known that the displacer is 90º out of phase with respect to the power piston, due to this fact information for the displacer can be obtained from the power piston measurements.

KINETCS OF A GAMMA-TYPE STIRLING ENGINE

As mentioned before the Stirling engine was coupled to a DC motor with an elastic band allowing the angular velocity of the engine not to be constant. This is induced due the counterweights connected to both pistons, these counterweights avoid that the engine stops when the pistons reach their critical positions. Figure 2 shows the counterweights used on this device. It is important to mention that the displacer has two counterweights while the power piston only has one counterweight.

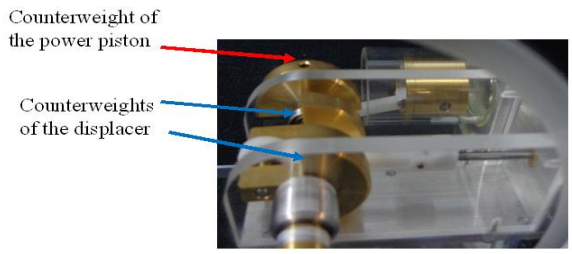

Figure 2 Counterweights attachment configuration in the Stirling engine used in this analysis.

Experimental data from the accelerometer is used; this data is presented in Figure 3; the data obtained by an integration procedure is also shown in Figure 3. This data is compared with the kinetic analysis of the Stirling engine. Equations (1-3) present the motion expressions for a Stirling engine. The position of the piston is obtained by Equation (1); Equation (2) is the time derivative of Equation (1), and finally Equation (3) is the second time derivative of Equation (1) or the first-time derivative of Equation (2).

$$x = r\,sin\,\theta + \sqrt{l^2 - r^2\,cos^2\,\theta} - \sqrt{l^2 - r^2} \tag{1}$$

$$u = \frac{dx}{dt} = r\omega\,cos\,\theta\left(1 + \frac{r\,sin\,\theta}{\sqrt{l^2 - r^2\,cos^2\,\theta}}\right) \tag{2}$$

$$a = \frac{d^2x}{dt^2} = \frac{du}{dt} = -r\omega^2\,sin\,\theta - \frac{r^2\omega^2\,sin^2\,\theta}{\sqrt{l^2 - r^2\,cos^2\,\theta}} + \frac{r^2\omega^2\,cos^2\,\theta}{\sqrt{l^2 - r^2\,cos^2\,\theta}}\left[1 - \frac{r^2\,sin^2\,\theta}{l^2 - r^2\,cos^2\,\theta}\right] \tag{3}$$

Figure 3a shows the comparison of the time evolution of the acceleration for the displacer obtained with the accelerometer and the theoretical acceleration, obtained by solving Equation (3). Relative maximum points are shown in the critical positions of the displacer with the experimental data (while in the theoretical analysis these points are not observed). This behavior is due to the fact that counterweights are attached to the end of the displacer. Thus, because of these mentioned positions; the counterweights allowed obtaining the maximum potential energy which is converted into kinetic energy enabling the piston to keep on moving without deaccelerating.

In Figure 3b the time evolution of the linear velocity for the displacer is presented. A comparison between the theoretical and experimental data is also presented. Although the angular velocity of the displacer is not constant the linear velocity presents good agreement with the theoretical linear velocity obtained by Equation (2), in which the angular velocity is considered constant. This behavior can be justified by the fact that the angular velocity of the DC motor is maintained constant, and that the counterweights contribute with small changes to the angular velocity but these are too small for directly affecting the total angular velocity. Also is important to mention that the constant velocity of the DC motor acts as a break for the displacer momentum, thus the angular velocity of the displacer is almost constant.

Figure 3c presents the comparison of the theoretical and experimental linear displacement of the displacer. The theoretical linear displacement is obtained by solving Equation (1). In this figure a good agreement is observed between the experimental and the theoretical data. It can be inferred that the small changes presented in the angular velocity and the acceleration due to the counterweights have not notorious effect on the displacement and linear velocity.

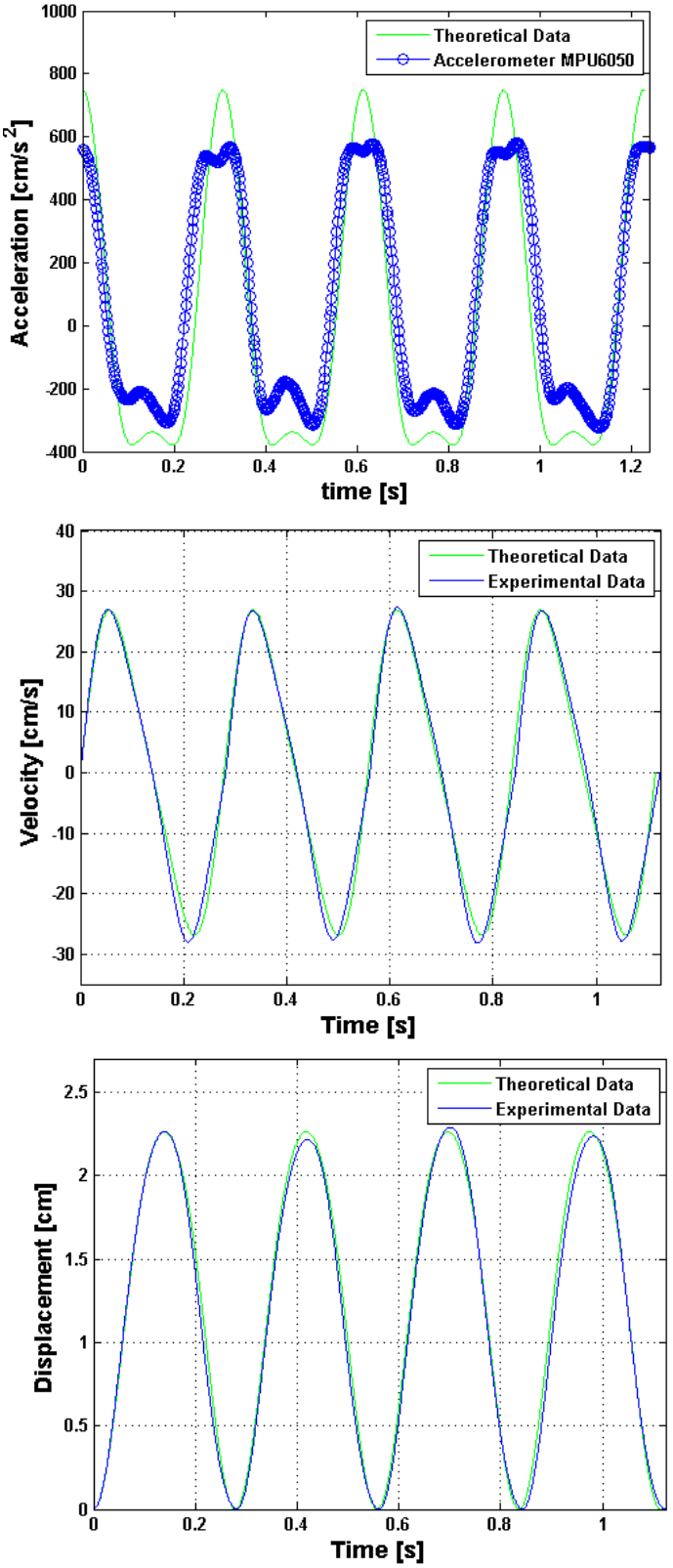

Figure 3 Theoretical vs experimental data comparison.

THERMODYNAMIC OF THE STIRLING ENGINE

Once the displacement of the displacer is known, it is possible to estimate the volume change inside the piston chamber. Also, the experimental measurements acquired by the pressure transducer enable to build a p-v diagram, presented in Figure 4.

Figure 4 shows that negative pressures are reached by the Stirling engine. These pressures are presented when the displacer is near its lower dead point. This is an expected behavior because the Stirling engine is operated as a heat pump, thus the displacer can be considered as an energy sink, extracting heat that is provided to the power piston.

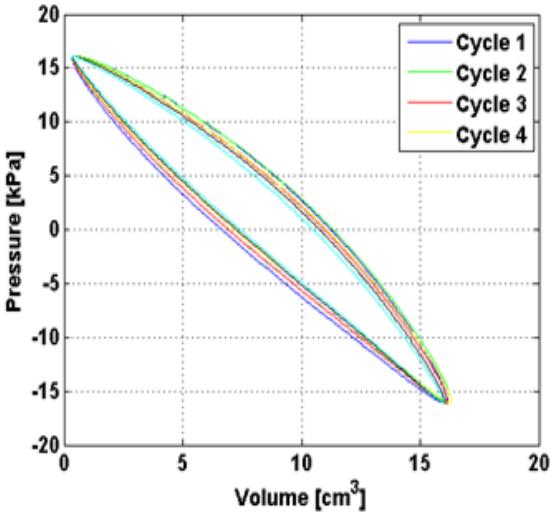

Figure 4 Pressure-volume diagram of the Stirling engine with a mean angular velocity of ω=200 rpm.

Figure 5 shows temperatures sensed at the critical positions of the displacer. The measurements were taken maintaining constant the temperature of the surroundings. The figure presents error bars that indicate the standard deviation of the measurements for every sensed point once the steady state is reached.

At the lower dead point the measured temperature having a mean angular velocity of 200 rpm is 30.2 ºC. If the angular velocity is increased a similar behavior is seen for temperature, and when the angular velocity reaches 300 rpm the temperature at the lower dead point is about 30.5 ºC. On the other hand, at the upper dead point a different behavior is observed: the temperature decreases by increasing the angular velocity. For example, the measured temperatures are 23.5 ºC for 200 rpm and 23 ºC for 300 rpm. This behavior is shown in Figure 5.

FLOW VISUALIZATION INSIDE THE DISPLACER

A fluid dynamics visualization was carried out inside the displacer. To obtain this visualization it is important to mention that the inlet and the outlet of the power piston are not collocated at the midpoint of the piston but they are located at the lateral region of the piston rod, as shown in Figure 6.

The technique implemented for the flow visualization used dry-ice tracker particles. These particles are injected inside de chamber of the Stirling engine through the pressure transducer (this position is shown in Figure 1). Once the particles are injected into the chamber the engine is turned on and operated enough time to assure that the flow is fully developed and it is possible to confirm that each cycle presents repeatability. The surrounding temperature is maintained constant at 23 ºC, thus it is possible to avoid dry-ice particles condensation for a longer period of time.

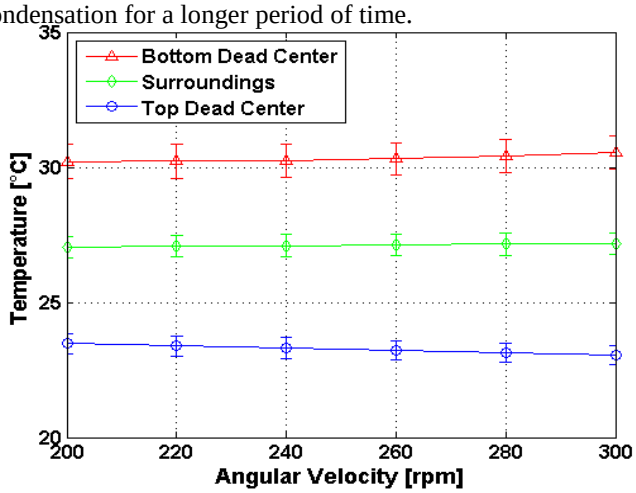

Figure 5 Temperature variation at the critical points of the displacer.

The experimental set up consists of a laser beam plane (Physics Reliant 150m, 457-514 nm wavelength) that is projected longitudinally through the displacer; this laser beam enters from the upper dead point and a rapid camera (Phantom Miro eX1) is installed perpendicular to the laser beam plane. As mentioned before, the steering wheel of the Stirling engine is driven by a DC motor. The flow visualizations were taken at a mean angular velocity of 200 rpm.

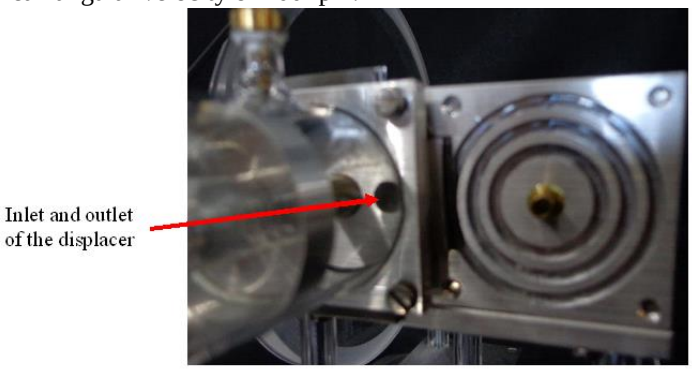

Figure 6 Air inlet/outlet position of the displacer.

The pictures analyzed were taken with a spatial resolution of 0.108 mm per pixel, while the temporal resolution was 0.001 s. The images were processed by means of the PIV technique with an interrogation area of 30 x 30 pixels and a 25% overlap.

Figure 7 shows some of the visualizations obtained with the PIV technique. These images were taken when the Stirling engine is operated as a heat pump with a constant angular

velocity of 200 rpm. The framework is located at the mid-point of the displacer when the piston is at its lower dead point; this consideration is imposed for a better interpretation of the results. The X-axis is considered on the horizontal direction and Y-axis is considered on the vertical direction.

Visualization techniques are extremely complex; several factors should be taken into account or the whole visualization could be not done right. In this case the results presented in Figure 7 show a white light beam passing through the piston chamber. This light beam interruption is due a little imperfection located at the tip of the piston chamber. This little imperfection promotes the light diffusion and causes the appearance of the white light beam.

The starting point selected for the analysis is the lower dead point of the displacer (θ=180º). When the displacer reaches this point a vacuum pressure is generated inside the piston chamber. Due to this, it is impossible to see the tracker particles from 180º ≤ θ ≤ 325º. Once the θ=370º position is reached the tracker particles are able to come back into the piston chamber.

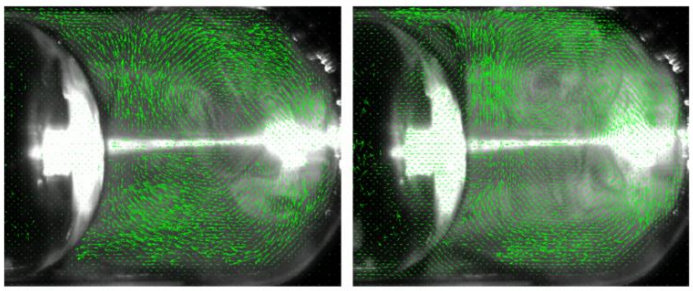

(a) $\theta = 0°$ (b) $\theta = 20°$

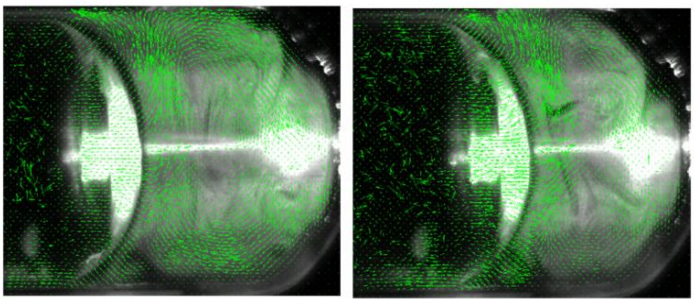

(c) $\theta = 40°$ (d) $\theta = 60°$

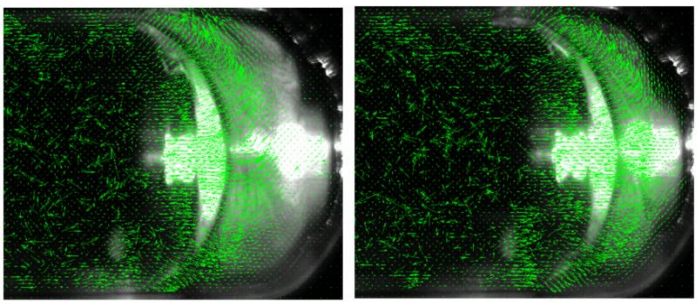

(e) $\theta = 80°$ (f) $\theta = 100°$

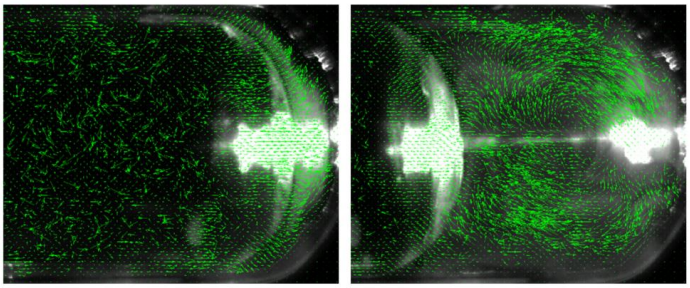

(g) $\theta = 120°$ (h) $\theta = 340°$

Figure 7 Fluid dynamic visualization inside the chamber of the displacer.

When the displacer reaches an angular position θ ≥ 325º, tracker particles are allowed to get into the chamber and they are now visible for the rapid camera.

The particles are highly noticeable mainly through the upper section of the displacer, as can be seen in Figure 7h. This injection of air-dry ice mixture generates a clockwise semi-toroidal vortex. In this figure it is possible to appreciate that the mid-point of the vortex is slightly displaced in the vertical direction, thus the middle point of the vortex is not centered with respect to the piston´s centerline. By a visual estimation, the center of the vortex is located at the position x= 11.0 mm, y= 2.3 mm.

At the position θ = 347º the exhaust process starts. A small portion of the fluid that entered the chamber (at θ = 325º) starts to evacuate the chamber between the upper region of the displacer and the piston skirt. The fluid keeps going out of the chamber until the displacer reaches the θ = 180º position. It is important to mention that the mid-point of the vortex is displaced while the displacer is moving along its chamber; when the displacer reaches the θ = 350º position the mid-point of the vortex is located at x= 10.9 mm, y=2.0 mm.

Once the displacer has reached the lower dead point (θ ≥ 0º), shown in Figure 7a, the mid-point of the vortex has been displaced to x= 10.7 mm, y= 3.1 mm, while a fraction of the fluid keeps going out of the chamber. Now the displacer starts moving along the upper dead point and the mid-point of the vortex will be displaced too. When the piston reaches the θ ≈ 38º position, two mid-points of the semi-toroidal vortex can be seen (surprisingly, these two points do not present symmetry with respect to the centerline of the displacer). Table 2 presents the transition of the mid-point of the vortex along the performed visualization.

As mentioned before the middle point of the vortex is displaced while the displacer is moving along its stroke. The upper mid-point of the vortex is displaced until the θ = 67º position and it will start to disappear. In other hand, when the displacer reaches the θ = 91° the lower mid-point of the vortex will start to disappear.

For all positions between 91º < θ < 180º the fluid inside the chamber of the displacer presents a laminar flow behavior. A fraction of the fluid is going out of the chamber of the displacer through the upper section while the rest of the fluid is displaced inside the chamber.

Table 2. Displacement of the vortex mid-point along the piston stroke.

θ[°]	Vortex middle point			
	Upper		Lower	
	x [mm]	y [mm]	x [mm]	y [mm]
325	11.0	2.3	-	-
350	10.9	2.0	-	-
0	10.6	3.0	-	-
10	8.7	5.0	-	-
20	7.8	5.9	-	-
30	8.0	6.2	-	-
38	8.2	6.4	10.5	-2.8
40	8.4	6.0	10.6	-2.8
50	9.9	6.2	10.9	-4.4
60	11.3	7.5	12.3	-5.8
67	12.2	9.2	13.2	-7.4
91	-	-	13.5	-8.4

CONCLUSIONS

In the present work the instrumentation of a Gamma-type U10050 Stirling engine is presented. This instrumentation allowed the correct measurement of important operating factors presented in the Stirling engines, as pressure variations, temperature, acceleration, velocity, and displacement, when the device is operated as a heat pump.

It was shown that the small angular velocity changes caused by the counterweights attached to the ends of the power piston and displacers are negligible. This implies that the displacement of the analyzed pistons is adequately determined by the equations of motions presented by Equations (1-3) so, it can be stated that this analysis could be carried out assuming a constant angular velocity.

Dry-ice tracker particles were used for the flow visualization and the implementations of the PIV technique. Velocity fields can be detected by the implementation of this technique. The visualization shows that a non-symmetrical semi-toroidal vortex is created when the displacer moves along the stroke line. The obtained images proved that the vortex is not symmetrical with respect to the centerline of the piston and that the mid-point of the vortex changes its locations while the displacer is moving. Several locations of the moving mid-point of the vortex were spotted and reported.

ACKNOWLEGGEMENTS

The authors gratefully acknowledge the support in the development of this work from the Renewable Energy Institute of the UNAM.

REFERENCES

[1] Mohammad H. Ahmadi, Mohammad Ali Ahmadi, Roham Bayat, Milad Ashouri, Michel Feidt, Thermo-economic optimization of Stirling heat pump by using non-dominated sorting genetic algorithm, Energy Conversion and Management, Volume 91, February 2015, Pages 315-322, ISSN 0196-8904.

[2] Ramla Gheith, Fethi Aloui, Sassi Ben Nasrallah, Determination of adequate regenerator for a Gamma-type Stirling engine, Applied Energy, Volume 139, 1 February 2015, Pages 272-280, ISSN 0306-2619.

[3] Manual: Stirling-Motor G U10050. https://www.a3bs.com/product-manual/U10050.pdf.

[4]Commercial web: https://www.3bscientific.com/physics,pg_83.html

[5] Mohsen jahanmiri, Particle image velocimetry: fundamentals and its application, Research report, Chalmers University of Technology, 2011, ISSN 1652-8549.

[6] Brian T. Love, Mark F. Reeder, Particle size control for PIV seeding using dry ice, 48th AIAA Aerospace Sciences Meeting Including the New Horizons Forum and Aerospace Exposition, 4 - 7 January 2010, Orlando, Florida.

[7] B. Greene, M. Reeder, J. Carfton, Characterizing dry ice particle response for clean seeding PIV applications, AIAA meeting papers on disc, (2008-3714), American Institute of Aeronautics and Astronautics, Reston, Va., 2008
ISSN: 10877215

[8] Melling, A., Tracer particles and seeding for particle image velocimetry, Meas. Sci. Tech., 1997, Vol. 8, pp.1406-1416

[9] Peter Scholz, Ilko Reuter, Dirk Heitmann, PIV measurements of the flow through an intake port using refractive index matching, 16th International Symposium on Applications of Laser Techniques to Fluid Mechanics, Lisbon, Portugal, 09-12 July, 2012.